

## Research Article



Metabolic Imaging

How to cite: Angew. Chem. Int. Ed. 2024, e202407349 doi.org/10.1002/anie.202407349

# In vivo Metabolic Sensing of Hyperpolarized [1-13C]Pyruvate in Mice Using a Recyclable Perfluorinated Iridium Signal Amplification by **Reversible Exchange Catalyst**

Jessica Ettedgui,\* Kazutoshi Yamamoto, Burchelle Blackman, Norikazu Koyasu, Natarajan Raju, Olga Vasalatiy, Hellmut Merkle, Eduard Y. Chekmenev, Boyd M. Goodson, Murali C. Krishna, and Rolf E. Swenson

Abstract: Real-time visualization of metabolic processes in vivo provides crucial insights into conditions like cancer and metabolic disorders. Metabolic magnetic resonance imaging (MRI), by amplifying the signal of pyruvate molecules through hyperpolarization, enables non-invasive monitoring of metabolic fluxes, aiding in understanding disease progression and treatment response. Signal Amplification By Reversible Exchange (SABRE) presents a simpler, costeffective alternative to dissolution dynamic nuclear polarization, eliminating the need for expensive equipment and complex procedures. We present the first in vivo demonstration of metabolic sensing in a human pancreatic cancer xenograft model compared to healthy mice. A novel perfluorinated Iridium SABRE catalyst in a fluorinated solvent and methanol blend facilitated this breakthrough with a 1.2-fold increase in [1-13C]pyruvate SABRE hyperpolarization. The perfluorinated moiety allowed easy separation of the heavy-metal-containing catalyst from the hyperpolarized [1-13C] pyruvate target. The perfluorinated catalyst exhibited recyclability, maintaining SABRE-SHEATH activity through subsequent hyperpolarization cycles with minimal activity loss after the initial two cycles. Remarkably, the catalyst retained activity for at least 10 cycles, with a 3.3-fold decrease in hyperpolarization potency. This proof-ofconcept study encourages wider adoption of SABRE hyperpolarized [1-13C]pyruvate MR for studying in vivo metabolism, aiding in diagnosing stages and monitoring treatment responses in cancer and other diseases.

#### Introduction

Traditional Magnetic Resonance (MR) techniques are constrained by sensitivity limitations, predicated upon small population differences across nuclear spin energy levels (10<sup>-6</sup>-10<sup>-5</sup>). Hyperpolarization methods such as dissolution Dynamic Nuclear Polarization (d-DNP)[1-3] enhance MR signals by amplifying nuclear spin polarization of the target spins, e.g., <sup>13</sup>C in [1-<sup>13</sup>C]pyruvate, enabling metabolic imaging of cancers and other diseases with abnormal metabolism (contributing to the Warburg effect). The leading hyperpolarized (HP) contrast agent, [1-13C]pyruvate, can also achieve rapid hyperpolarization through a cost-effective method: SABRE-SHEATH (Signal Amplification By Reversible Exchange in SHield Enables Alignment Transfer to Heteronuclei)<sup>[4-6]</sup> by employing parahydrogen (p-H<sub>2</sub>) as a source of polarization and an iridium catalyst for polarization transfer via the process of simultaneous chemical exchange of p-H<sub>2</sub> and to-be-hyperpolarized substrates on a metal center.<sup>[7,8]</sup> The initial exploration of hyperpolarizing [1-13C]pyruvate through SABRE-SHEATH was introduced by Duckett et al. [9] and subsequently refined by others. [10–12] The HP state in pyruvate can be achieved in a minute via SABRE-SHEATH versus approximately 1 hour for d-DNP, and at a small fraction of the cost. While progress has been made with demonstrating recycling of some heterogeneous

[\*] Dr. J. Ettedgui, Dr. B. Blackman, Dr. N. Raju, Dr. O. Vasalatiy, Dr. R. E. Swenson

Chemistry and Synthesis Center

National Heart, Lung, and Blood Institute

9800 Medical Center Drive, Rockville, Maryland 20850, United

E-mail: jess.benjamini-ettedgui@nih.gov

Dr. K. Yamamoto, Dr. N. Koyasu, Dr. M. C. Krishna Center for Cancer Research

National Cancer Institute

Bethesda, 10 Center Drive Maryland 20814, United States

National Institute of Neurological Disorders and Stroke Bethesda, 10 Center Drive Maryland 20814, United States Prof. Dr. E. Y. Chekmenev

Department of Chemistry, Integrative Biosciences (Ibio), Karmanos Cancer Institute (KCI), Wayne State University,

Detroit, Michigan 48202, United States

Prof. Dr. B. M. Goodson

School of Chemical & Biomolecular Sciences and Materials

Technology Center, Southern Illinois University,

Carbondale, Illinois 62901, United States

© 2024 Wiley-VCH GmbH. This is an open access article under the terms of the Creative Commons Attribution License, which permits use, distribution and reproduction in any medium, provided the original work is properly cited.

catalysts, [13-15] to date all SABRE methodologies capable of generating HP [1-13C]pyruvate biocompatible solutions have only employed SABRE catalysts in single-use modes. Nevertheless, Ir is an expensive metal (>\$160/g in pure form and substantially greater in organometallic compounds), and preparing a clinical dose of HP [1-13C]pyruvate (~1 g) will likely require over 0.1 g Ir. Therefore, SABRE catalyst recycling is greatly desirable to decrease the cost associated with future clinical-scale production and improve sustainability. Moreover, catalyst recycling mitigates the need for initial activation of the SABRE catalyst, potentially allowing substantially faster repetition of the hyperpolarization cycle. Despite the considerable translational benefits of SABRE, there are toxicity concerns associated with the utilization of organic media and the heavy-metal-containing SABRE catalysts, which are typically based on iridium.<sup>[7,8]</sup> Significant efforts have been made to optimize the extraction of HP pyruvate following SABRE-SHEATH, with the ambition of providing safe biocompatible solutions for in vivo applications. Those efforts involve refining techniques such as: CASH-SABRE, [16] whereby the principles of phasetransfer catalysis were used to improve the SABRE response in water while simultaneously achieving catalyst separation; or HET-SABRE, [13-15,17,18] where catalyst complexes are immobilized on solid supports; and more recently Re-D SABRE,[12] which is based on rapid pyruvate precipitation followed by a phase separation. Recently another methodology, using fast solvents evaporation under heating, yielded biocompatible solutions that have been successfully employed for metabolic imaging HP [1-13C]pyruvate in vivo. [19,20] This purification Scheme reported methanol levels suitable for preclinical studies, but the Iridium content remained high.

Heavily fluorinated metal complexes, i.e., containing perfluorinated carbon-tailed ligands, have distinct properties—such as enhanced hydrophobicity. These properties are often leveraged for catalyst removal in fluorous biphasic catalysis, extraction, and recovery through fluorous solid-phase extraction. [21–23] Importantly, the metal content is drastically reduced in the corresponding products. [24,25]

Our present work showcases the feasibility of efficient SABRE catalyst recycling and re-use, coupled with the efficacy of utilizing fluorinated solvents to enhance hyperpolarization levels compatible with in vivo sensing, while addressing the need for efficient iridium removal, marking significant progress towards translational research in metabolic imaging.

#### **Results and Discussion**

### Perfluorinated SABRE Catalyst in Fluorinated Solvent

SABRE-SHEATH hyperpolarization was conducted in a mixture of methanol and hydrofluoroether (HFE) solvent with DMSO as a co-ligand, providing [1- $^{13}$ C]pyruvate  $^{13}$ C polarization ( $P_{13C}$ ) of up to 16%. The 1.2-fold  $P_{13C}$  boost (compared to methanol solvent) was attributed to the fluorinated solvent's increased gas solubility, [ $^{26-28}$ ] Figure S1.

Increased p-H<sub>2</sub> availability within the solution enhances polarization transfer, thus improving SABRE-SHEATH efficiency. Briefly, the SABRE-SHEATH hyperpolarization process utilized 35 mM sodium [1-13C]pyruvate, 6 mM perfluorinated SABRE pre-catalyst [IrCl(COD)(f-sIMes)](f-IsMes = trans-4,5-Bis(3,3,4,4,5,5,6,6,7,7,8,8,8-tridecafluorooctyl)-1,3-bis(2,4,6-trimethylphenyl)dihydroimidazol-2-ylidene; COD = cyclooctadiene) and 56 mM DMSO in a 0.5-mL mixture of CD<sub>3</sub>OD and the hydrofluoroether Novec<sup>TM</sup> fluid 7100 (3:2), utilizing a microtesla apparatus MATRESHCA (XeUS Technologies LTD, Nicosia, Cyprus) tailored for the SABRE-SHEATH studies.<sup>[29]</sup> Activation (approximately 15 to 20 minutes) was conducted under 20 standard cubic centimeters per minute (sccm) low flow of p-H2 to prevent solvent evaporation, Figure S2. The optimum microtesla magnetic field and temperature for efficient polarization transfer is achieved at approximately  $0.4 \,\mu\text{T}$  and  $-5\,^{\circ}\text{C}$ , respectively, Figure S4.

Overall, the mixture of CD<sub>3</sub>OD and HFE solvents accelerates the relaxation dynamics of [1-13C]pyruvate as compared to a deuterated methanol solution only (Figure 1c). [30-32] More specifically, as observed in Figures 1d, 1e, the  $P_{13C}$  build-up time constant  $(T_b)$  for (bound + free) species in the shield was shorten to  $T_b = 4.7 \pm 1.0$  s, and the relaxation time in the shield was measured to be  $T_1 = 12.6 \pm$ 1.1 s—faster than in methanol alone with either perfluorinated and unmodified SABRE catalysts. At 1.88 T, the relaxation slowed significantly, giving a decay constant of  $66.5 \pm 3.6$  s. Remarkably, at Earth's field the relaxation dynamics were notably faster when using the perfluorinated SABRE catalyst in the CD<sub>3</sub>OD/HFE solvent mixture and T<sub>1</sub> value at Earth's field was measured to be  $9.3 \pm 0.8 \, \mathrm{s}$  (Figure 1e). The precise origin of the accelerated relaxation at low magnetic fields remains unclear, but it may be attributed to a combination of more efficient cross-relaxation with nuclear spins (and possibly, residual electronic spins) under these low-field conditions.[33] Additionally, the increased effective molecular weight of the perfluorinated catalyst (> 1400 g/mol) may play a role, potentially involving the formation of macromolecular assemblies with the fluorinated solvent. Indeed, slower molecular motion within low magnetic fields, e.g. those encountered in the Earth's magnetic field, could result in more efficient relaxation dynamics. Similar observations have been documented in peptides and proteins with molecular weights surpassing 1000 Da.[34,35] Although experimental evidence for macromolecular assembly formation is currently lacking, it is plausible that the existence of larger macromolecular assemblies involving the fluorinated solvent would enhance this phenomenon.

#### Biphasic Extraction For Catalyst Recycling

In addition to increasing the p-H<sub>2</sub> concentration in solution, fluorinated solvents exhibit negligible miscibility with water (solubility of Novec<sup>TM</sup> fluid 7100 solvent in water is 12 ppmw —parts per million by weight) and low toxicity. [36] Once optimal polarization parameters were determined, we

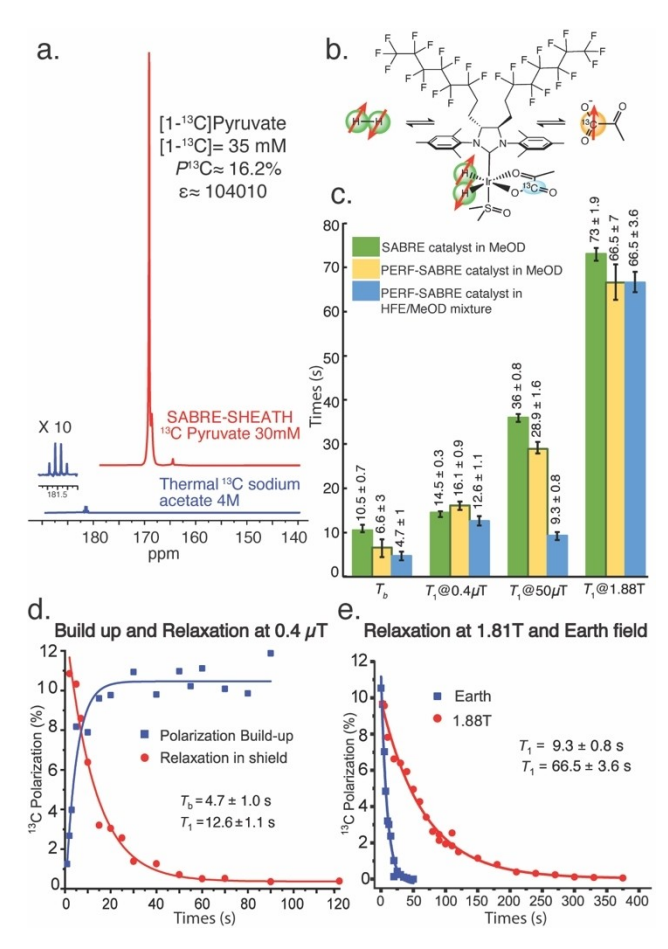


Figure 1. (a) Representative HP <sup>13</sup>C spectrum of 35 mM sodium [1-<sup>13</sup>C]pyruvate with 6 mM perfluorinated SABRE pre-catalyst and 56 mM DMSO in a 0.5 mL mixture of CD<sub>3</sub>OD and Novec<sup>™</sup> fluid 7100 obtained by performing SABRE-SHEATH at 0°C, and the corresponding <sup>13</sup>C spectrum of thermally polarized sodium [1-13C]acetate used for reference. (b) Schematic of perfluorinated SABRE-SHEATH hyperpolarization process for [1-13C]pyruvate. (c) Histogram of the relaxation times of <sup>13</sup>C hyperpolarization under SABRE-SHEATH conditions with the original SABRE catalyst IrIMes and the perfluorinated SABRE catalyst. The relaxation times are measured in two different solvents: CD<sub>3</sub>OD and a mixture of CD<sub>3</sub>OD and HFE; and at different fields: 0.4  $\mu T,\,50~\mu T$  (earth field), and at 1.88 T (the NMR detection field).  $^{[30\text{-}32]}$ (d) Total (bound + free) 13C polarization buildup and decay at  $B_{\textit{transfer}}\!=\!0.4~\mu\text{T}$  and  $T_{\textit{transfer}}\!=\!-5\,^{\circ}\text{C}.$  (e) Total (bound+free)  $^{^{1}3}\text{C}$  polarization decay at 50 µT (earth field), and at 1.88 T (the NMR detection

leveraged those attributes and applied principles of phasetransfer catalysis by enhancing SABRE response in the water phase while achieving catalyst separation, Figure 2. In the implementation of this approach a sample consisting of 35 mM sodium [1-13C]pyruvate, 6 mM perfluorinated catalyst, and 56 mM DMSO in a mixture of 0.3 mL CD<sub>3</sub>OD and 0.2 mL NovecTM fluid 7100 was utilized. Following perfluorinated catalyst activation with p-H2, the sample was placed in the mu-metal shield to facilitate the SABRE-SHEATH [1-13C]pyruvate polarization. Subsequently, 0.3 mL of D<sub>2</sub>O was introduced into the hyperpolarized solution to allow the separation of the organic fluorinated phase containing the catalyst, and the aqueous phase containing the hyperpolarized [1-13C]pyruvate. Unfortunately, the addition of water resulted in the emulsification of the phases. Despite showing no loss in hyperpolarization, this emulsification rendered the phase-transfer catalysis method impractical due to the extended phase separation time exceeding 10 minutes. Once the aqueous phase is separated, it remained colorless, and the iridium content of the aqueous fraction was determined to be only  $673 \pm 160$ ppb in 2 samples. Nevertheless, this result shows the great ability of this approach to sequester the catalyst away from the substrate. To accelerate the separation of the emulsion, the volume of fluorinated solvent was increased and the utilization of a fluorinated co-ligand such phenyltrifluoromethyl sulfoxide (PTMSO) was preferred to DMSO. The change in co-ligand type led to minor changes in the optimal polarization transfer conditions (see Supporting Information p8). While the optimum magnetic field stayed at 0.4 µT, the optimum temperature for HP pyruvate with PTMSO is drastically shifted to  $T_{\scriptscriptstyle T}$  between 25 and 30°C. As previously reported, temperature exerts a profound influence on the exchange rates of [1-13C]pyruvate on SABRE catalyst.<sup>[11,30-32]</sup> A temperature sweep with the perfluorinated catalyst, coupled with PTMSO as a co-ligand, revealed a different distribution among the key SABRE species, [30] in contrast to using DMSO as a co-ligand, Figure S9.

It should be noted that the maximal [1-13C]pyruvate polarization levels attained reached up to 14.4 % when using the perfluorinated SABRE catalyst and PTMSO as a coligand in a mixture of methanol and HFE, corresponding to a signal enhancement ( $\epsilon$ ) of approximately 92,000-fold. This enhancement was slightly lower compared to the enhancement achieved when using DMSO as the co-ligand (104010-fold). Despite our optimization efforts, the polarization levels achieved with PTMSO never reached those attained with DMSO.

As observed earlier, the relaxation dynamics of [1-13C]pyruvate are shorter in a methanol/HFE solvent mixture, the total  $P_{13C}$  (bound+free) build-up time is  $T_b = 8.9 \pm 2.5$  s compared to the corresponding  $T_{\rm 1}$  value in shield of 18.0  $\pm$ 0.8 s. T<sub>1</sub> values at both earth field and 1.88 T were measured at  $14.9 \pm 1.0$  s and  $59.0 \pm 8.1$  s, respectively, thus explaining the slightly lower P<sub>13C</sub> values obtained in a mixture of methanol and HFE.

Once the SABRE-SHEATH hyperpolarization conditions for the perfluorinated SABRE catalyst were optimized with PTMSO as the co-ligand (SI), we applied the catalyst phase-transfer technique using biphasic extraction to isolate the HP [1-13C]pyruvate in an aqueous solution, as described in Figure 2. SABRE-SHEATH hyperpolarization was performed at a 0.4 µT field and 25 °C (Figure 2a) on samples containing 28 mM sodium [1-13C]pyruvate, 5 mM perfluorinated SABRE catalyst, and 97 mM PTMSO in 0.3 mL CD<sub>3</sub>OD and 0.3 mL of 7100 Novec<sup>TM</sup> solvent and were depressurized after being promptly transferred to a 1.88 T spectrometer. A subsequent addition of 0.3 mL of D<sub>2</sub>O facilitated the perfluorinated catalyst phase transfer separation, requiring approximately ~15 s for complete sample 5213773, 0] Downloaded from https://onlinelibrary.wiley.com/doi/10.1002/anie.202407349 by Readcube (Labtiva Inc.), Wiley Online Library for not consistency for not co

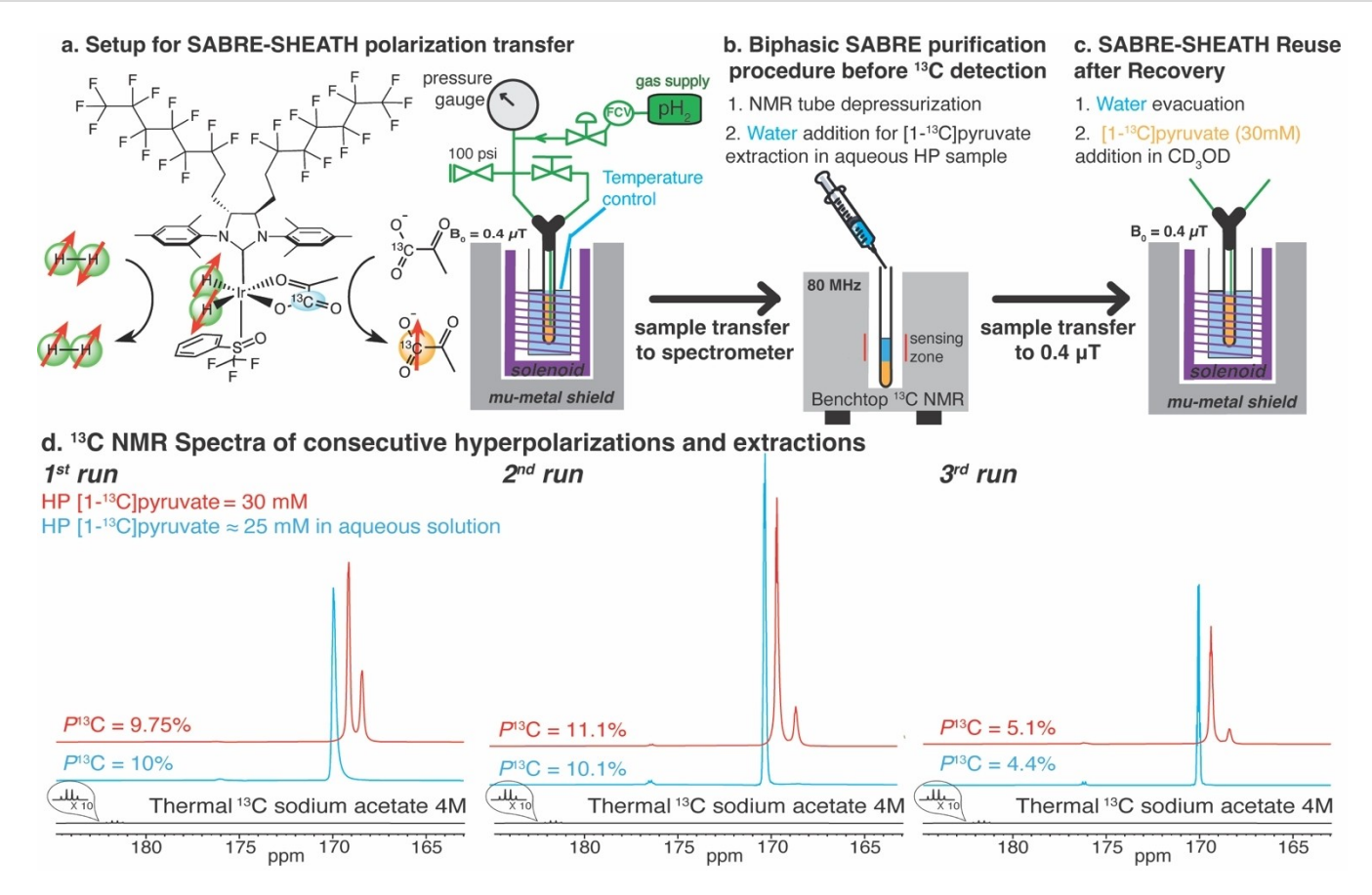


Figure 2. Schematic of perfluorinated SABRE-SHEATH setup, followed by biphasic pyruvate extraction and reuse of the perfluorinated SABRE catalyst. (a) A 5 mm NMR tube is pressurized with ~8 bar p-H2 flowing through the sample at a fixed flow rate. The samples contained 30 mM [1-13C]pyruvate, 5 mM catalyst, and 98 mM PTFMSO as a co-ligand in a mixture of HFE and CH<sub>2</sub>OD. Hyperpolarization occurred within a mu-metal shielded electromagnet, with the magnetic field adjusted to approximately  $B_{transfer} \approx 0.4 \, \mu T$  and  $T_{transfer}$  set at 20 °C. (b) After 30 s of p-H<sub>2</sub> bubbling, the sample is transferred to the spectrometer (B = 1.88 T), depressurized, and 0.3 mL of water is added to the sample, which allows the extraction of [1-13C]pyruvate from the fluorinated phase. (c) The recovery and reuse of the perfluorinated catalyst consists of evacuating the aqueous phase and adding a freshly prepared methanol solution containing 30 mM [1-13C]pyruvate to the fluorinated phase containing the perfluorinated catalyst. The samples are hyperpolarized in the mu-metal shield with the same catalyst used previously. The extraction step is repeated a second time as described in step b and the polarization level of [1-13C]pyruvate is measured after extraction. (d) 13C NMR spectra of [1-13C]pyruvate in a mixture of HFE and CD<sub>3</sub>OD before and after extraction of the first 3 extractions recycle and reuse of the same perfluorinated catalyst.

preparation, Figure 2b. This process resulted in a visibly two-phase sample separation, one yellow organic phase at the bottom of the NMR tube containing the catalyst, and another clear aqueous phase containing the hyperpolarized [1-13C]pyruvate. The NMR spectrum of the aqueous phase was acquired by aligning it with the spectrometer's sensing zone through NMR position adjustment.

The initial polarization of the HP [1-13C]pyruvate signal in organic solvents was  $P_{13C}$  of ~9.75 %, corresponding to an enhancement of  $\varepsilon$  ~60,235. After water addition and phase separation, the HP [1-13C]pyruvate signal in the aqueous fraction was measured to be ~10%, corresponding to an enhancement of  $\varepsilon$  ~61,750. Furthermore, the residual levels of organics in the aqueous fraction were measured using LCMS methods (Table S1) and pyruvate concentration was evaluated at  $25.3 \pm 5.5$  mM in the aqueous media. To assess catalyst removal, Ir elemental content in the aqueous [1-13C]pyruvate solution was analyzed using inductively coupled plasma Mass Spectroscopy (ICP-MS) and revealed an average residual Ir concentration of only 542 ± 212 ppb across 6 samples.

Additionally, we investigated the potential reusability of the fluorinated phase, containing the activated perfluorinated catalyst, for subsequent cycles of SABRE-SHEATH hyperpolarization. The aqueous phase containing the pyruvate is evacuated and a newly prepared solution, consisting of about 30 mM sodium [1-13C]pyruvate in 0.3 mL CD<sub>3</sub>OD, was introduced into the previously used fluorinated phase containing the perfluorinated catalyst (Figure 2c). A subsequent round of SABRE-SHEATH hyperpolarization was executed, and within 15 minutes, the initial [1-13C]pyruvate polarization level was re-attained, yielding  $P_{13C} \approx 11.1$  %. A second water-phase extraction, consistent with the procedure outlined in Figure 2b, resulted in [1-13C]pyruvate polarization levels up to of  $P_{13C}$  of ~10.1%. Thus, the biphasic separation method employing perfluorinated catalyst exhibited good recyclability, preserving its activity through successive [1-13C]pyruvate hyperpolarization cycles. After 5213773, Q. Downloaded from https://onlinelibrary.wiley.com/doi/10.1002/anie.2024/07349 by Rededbe (Labtiva Inc.), Wiley Online Library on [06/10/2024]. See the Terms and Conditions (https://onlinelibrary.wiley.com/terms-and-conditions) on Wiley Online Library for rules of use; OA articles are governed by the applicable Creative Commons License

the initial two cycles of catalyst recovery and reuse, there is a subsequent 2.2-fold  $P_{13C}$  decrease observed on the third cycle, with a polarization level of ~5.1 %, after 15 min of p-H<sub>2</sub> bubbling. The third water-phase extraction resulted in [1- $^{13}$ C]pyruvate polarization levels of  $P_{13C}$  of ~4.4%. Notably, the catalyst remained active for a minimum of 10 cycles, despite experiencing a 3.3-fold reduction in hyperpolarization potency using the present manual equipment setup. We believe that automation can substantially improve the recycling process, rendering faster repeat cycles and greater SABRE catalyst potency retention through the repeat cycles. Moreover, additional fine-tuning of chemical structure of the fluorinated co-ligand of the SABRE catalyst holds potential for further enhancement in <sup>13</sup>C polarization levels. The incorporation of automation into this manual and labor-intensive procedure is anticipated to reduce iridium contamination, enhance operational efficiency, and consequently, elevate polarization levels.

#### In Vivo Sensing

Our aim was to demonstrate the potential of the developed mixture for facilitating metabolic sensing applications in vivo. For the in vivo experiments, DMSO was chosen as the co-ligand based on three primary considerations. Firstly,

DMSO demonstrated higher polarization levels in a methanol and HFE solvent blend. Secondly, the purification of hyperpolarized [1-13C]pyruvate aqueous solutions for in vivo applications has been demonstrated for SABRE applications by Schmidt et al.[19] Lastly, the established toxicity profile of DMSO aligns with its compatibility for in vivo applications, while it is unknown for phenyl trifluoromethyl sulfoxide (PTMSO). In our study, we conducted experiments using a 3T preclinical MRI system to assess the efficacy of the newly developed mixture in achieving suitable levels of [1-13C]pyruvate hyperpolarization for in vivo metabolic sensing. These in vivo experiments involved investigations on both healthy nude mice and MIA PaCa-2 human pancreatic tumor-xenografts. (Figure 3). For those experiments, we used a recently reported protocol [19,37] that involves addition of a Trizma buffer (adapted for physiological conditions ~7.4 pH with 40 mM Trizma buffer, 50 mM NaCl and 0.27 mM EDTA) to a SABRE-SHEATH polarized solution, followed by vacuum evaporation (for 10 s) under heating (95 °C). As fluorinated solvents have a lower boiling point the solvent evaporation is fast. The purification procedure was performed at 50 mT, in the vicinity of the MRI, in order to reduce T<sub>1</sub> losses. The HP samples consisted of 35 mM sodium [1-13C]-pyruvate, 6 mM perfluorinated catalyst, and 56 mM DMSO in a mixture of CD<sub>3</sub>OD and NovecTM fluid 7100 (3:2) pressurized with

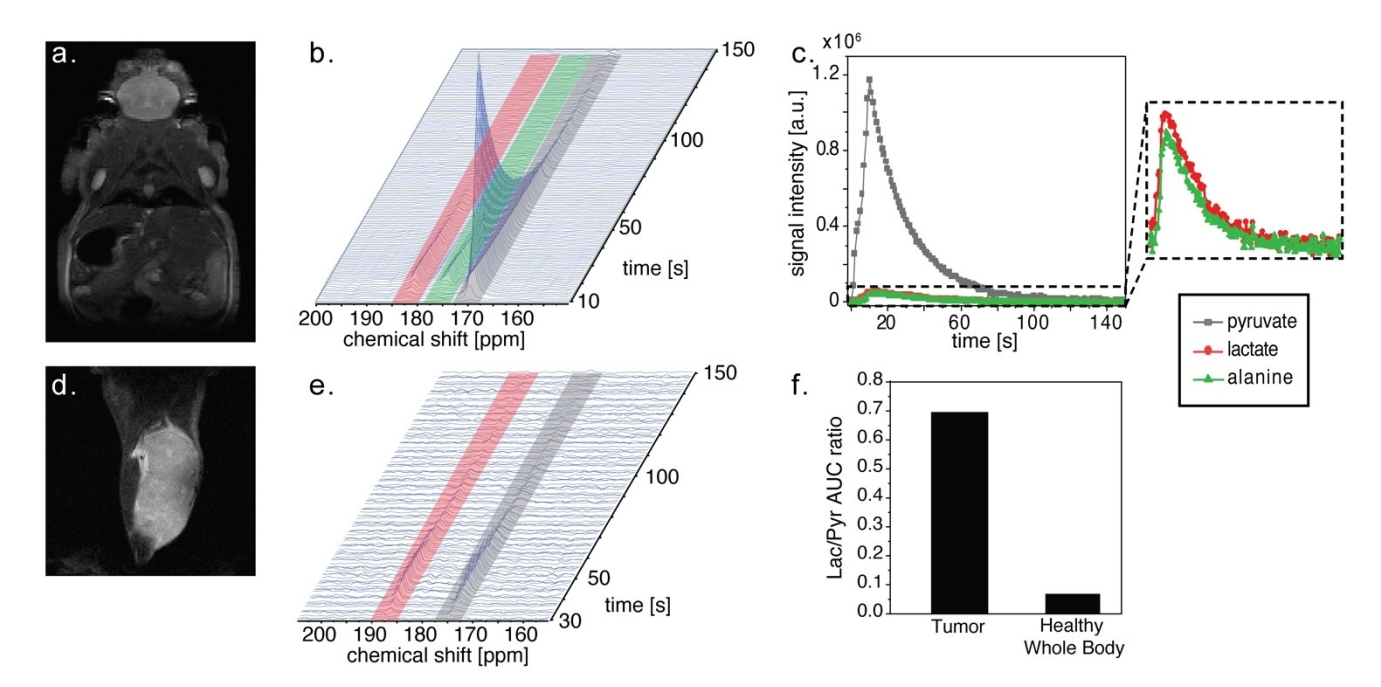


Figure 3. SABRE-SHEATH hyperpolarization of [1-13C]-pyruvate sensitively detects site specific metabolism in vivo (a)  $T_2$ -weighted <sup>1</sup>H MRI of the body mouse's body. (b) Dynamic hyperpolarized 13C-MR spectroscopy demonstrated in the whole body of a healthy mouse after hyperpolarized [1-13C]-pyruvate injection using a whole-body detection coil. (c) Time-dependent metabolic spectroscopy of [1-13C] pyruvate (grey) can depict enzymatic conversions into [1-13C] lactate (red) and [1-13C] alanine (green). Inset: The Time-dependent metabolism of [1-13C] pyruvate via enzymatic conversion into [1- $^{13}$ C]lactate and [1- $^{13}$ C]alanine observed in the whole body spectroscopy. (d)  $T_z$ -weighted  $^1$ H MRI of the xenografts embedded MIA PaCa-2 tumor cell lines into the right hind legs of athymic nude mice using a 17 mm diameter home-built 13C solenoid coil with a saddle 1H coil. (e) Aberrant in vivo metabolism in the tumor region was observed via hyperpolarized <sup>13</sup>C dynamic spectra mouse leg xenografts of MIA PaCa-2. (f) The lactate to pyruvate AUC (Area Under the Curve) ratios in the tumor regions and the whole healthy mouse body. The spectra were acquired every 1 s for 300 s on a 3T MRI scanner. [1-13C]-pyruvate peak (170 ppm) was observed as well as its conversion into lactate (185 ppm). Dynamic <sup>13</sup>C MRS were processed on MATLAB with a home-made script utilizing a singular value decomposition based low rank denoising method. <sup>[38]</sup>

5213773, 0] Downloaded from https://onlinelibrary.wiley.com/doi/10.1002/anie.202407349 by Readcube (Labtiva Inc.), Wiley Online Library for not consistency for not co

pH<sub>2</sub> at 110 psi. The activation was done at 20 sccm for

20 min at room temperature, while the [1-13C]-pyruvate SABRE-SHEATH polarization transfer was done in a mumetal shield at 0.4 mT and 150 sccm p-H<sub>2</sub>, between - 5 and 0°C. The solutions of HP [1-13C]-pyruvate were subjected to the purification method, which consisted in buffer addition, solvent evaporation and filtration (Oasis® PRIME HBL Plus light 100 mg filter) to remove the precipitated catalyst. The residual iridium content in those solutions was approximately 390  $\pm$  235 ppb (measured by ICP-MS) after filtration in 6 samples. The preparation of the HP solutions took approximately 35 sec and were immediately injected through a tail vein cannula of a mouse placed in a double tuned <sup>1</sup>H/<sup>13</sup>C coil. The <sup>13</sup>C signal was monitored every 1 s using the 3T MRI scanner with a 10-degree flip angle pulse.

The [1-13C]-pyruvate signal was detected in the mouse body and tumor-xenografts MIA PaCa-2 immediately after its injection and stayed detectable for more than 60 and up to 120 seconds (Figure 3b) as well as the predominant [1-13C]-lactate signal in the tumor. Figure 3f shows the lactate to pyruvate AUC ratios indicate that elevated lactate productions can be observed in the tumor regions compared to the whole body. It is noteworthy that the animals utilized for the MR spectroscopy presented in Figure 3 successfully survived the procedures. Generally, to ensure successful outcomes with high survival rates, meticulous execution of filtration and evaporation processes is imperative. Our research group is actively addressing safety concerns, including the determination of the median lethal dose (LD50), to further enhance the experimental protocols. To the best of our knowledge, this is the first example of SABRE-SHEATH hyperpolarization methodologies to detect dynamic altered in vivo metabolisms in a disease model and in a tumor xenograft in particular. Considering the relatively flexible applicability on various hyperpolarizing probes, which SABRE-SHEATH provides, these experimental results can be one of the milestones for the future applications in preclinical and clinical settings. Although the peak intensities remain low, this trial conducted in live organisms was a proof-of-concept and provided strong evidence supporting the use of SABRE-SHEATH polarized pyruvate for metabolic imaging, highlighting its effectiveness in monitoring dynamic metabolic processes within living organism systems and tumors. We hypothesize that optimization of other aspects of the SABRE process can further enhance the  $P_{13C}$  values that can be achieved for the produced HP [1-13C]pyruvate. For example, the utility of deuterated [1-13C]pyruvate and pulsed SABRE-SHEATH Schemes has the potentially to nearly double  $P_{13C}$ . [19,39]

#### Conclusion

In summary, we demonstrated efficient SABRE-SHEATH hyperpolarization for production of biocompatible aqueous solutions of HP [1-13C]pyruvate with minimal iridium contamination using the perfluorinated catalyst, which also allows a 1.2-fold greater  $P_{13C}$  when using fluorinated solvents. Through meticulous co-ligand selection, the integrity of the catalyst's functionality across multiple iterations remains intact, as demonstrated by the repetitive hyperpolarization and extraction cycles of HP [1-13C]pyruvate. Given the clinical dose requirement of HP [1-13C]pyruvate, SABRE catalyst recycling becomes imperative to mitigate costs, particularly as clinical-scale production may necessitate large quantities of iridium. Furthermore, catalyst recycling facilitates faster hyperpolarization cycles and automation. The findings from the in vivo study demonstrated the effectiveness of using SABRE-SHEATH polarized pyruvate in fluorinated solvents for metabolic sensing in MIA PaCa-2 xenograft tumors, affirming its capability to monitor the dynamic metabolic processes occurring within both healthy and pathological tissues in living organisms. This marks the first application of SABRE-SHEATH hyperpolarization techniques for detecting dynamically altered in vivo metabolisms within a disease model. This combination of low iridium content and catalyst recycling potentially allows SABRE to transition for routine low-cost clinical use. SABRE-SHEATH utilizing the perfluorinated SABRE catalyst emerges as an appealing, cost-effective alternative to d-DNP for preparing bio-compatible HP [1-13C]pyruvate formulations in next-generation molecular imaging.

#### **Supporting Information**

Please find additional experimental details, materials, and sample characterization. The authors have cited additional references within the Supporting Information. [40,41]

#### **Acknowledgements**

E.Y.C. and B.M.G. acknowledge support from the NSF under grants CHE-1904780, CHE-1905341, and NIBIB R21 EB033872. We thank Shiraz Nantogma and Isaiah Adelabu for their help with preparation of parahydrogen gas. We thank Drs. Andreas Schmidt and Henri De Maissin for their insightful conversation on the purification steps.

#### **Conflict of Interest**

J.E., R.S., R.N., and M.K. are inventors on a National Institutes of Health patent application on this work (U.S. Patent Application No. 63/328,545, filed 4/7/2022). B.M.G. and E.Y.C. declare stake ownership in XeUS Technologies, LTD. E.Y.C. declares stake ownership in VLS.

#### **Data Availability Statement**

The data that support the findings of this study are available in the supplementary material of this article.



**Keywords:** Hyperpolarized MRI · Parahydrogen · SABRE-SHEATH · Metabolic sensing · Catalyst Reuse and Recycling

- [1] J. H. Ardenkjær-Larsen, B. Fridlund, A. Gram, G. Hansson, L. Hansson, M. H. Lerche, R. Servin, M. Thaning, K. Golman, *Proc. Natl. Acad. Sci. USA* 2003, 100, 10158–10163.
- [2] K. H. Hausser, D. Stehlik, Adv. Magn. Opt. Reson. 1968, 3, 79–139.
- [3] A. Abragam, M. Goldman, Rep. Prog. Phys. 1978, 41, 395-467.
- [4] R. V. V. Shchepin, M. L. Truong, T. Theis, A. M. Coffey, F. Shi, K. W. W. Waddell, W. S. Warren, B. M. Goodson, E. Y. Chekmenev, J. Phys. Chem. Lett. 2015, 6, 1961–1967.
- [5] M. L. L. Truong, T. Theis, A. M. Coffey, R. V. Shchepin, K. W. Waddell, F. Shi, B. M. Goodson, W. S. S. Warren, E. Y. Chekmenev, J. Phys. Chem. C 2015, 119, 8786–8797.
- [6] T. Theis, M. L. Truong, A. M. Coffey, R. V. Shchepin, K. W. Waddell, F. Shi, B. M. Goodson, W. S. Warren, E. Y. Chekmenev, J. Am. Chem. Soc. 2015, 137, 1404–1407.
- [7] M. J. Cowley, R. W. Adams, K. D. Atkinson, M. C. R. Cockett, S. B. Duckett, G. G. R. Green, J. A. B. Lohman, R. Kerssebaum, D. Kilgour, R. E. Mewis, J. Am. Chem. Soc. 2011, 133, 6134–6137.
- [8] R. W. Adams, J. A. Aguilar, K. D. Atkinson, M. J. Cowley, P. I. P. Elliott, S. B. Duckett, G. G. R. Green, I. G. Khazal, J. Lopez-Serrano, D. C. Williamson, *Science* 2009, 323, 1708–1711.
- [9] W. Iali, S. S. Roy, B. J. Tickner, F. Ahwal, A. J. Kennerley, S. B. Duckett, *Angew. Chem. Int. Ed.* **2019**, *58*, 10271–10275.
- [10] B. Chapman, B. Joalland, C. Meersman, J. Ettedgui, R. E. Swenson, M. C. Krishna, P. Nikolaou, K. V. Kovtunov, O. G. Salnikov, I. V. Koptyug, M. E. Gemeinhardt, B. M. Goodson, R. V. Shchepin, E. Y. Chekmenev, *Anal. Chem.* 2021, 93, 8476–8483.
- [11] I. Adelabu, P. TomHon, M. S. H. Kabir, S. Nantogma, M. Abdulmojeed, I. Mandzhieva, J. Ettedgui, R. E. Swenson, M. C. Krishna, B. M. Goodson, T. Theis, E. Y. Chekmenev, ChemPhysChem 2022, 23, e202100839.
- [12] A. B. Schmidt, H. De Maissin, I. Adelabu, S. Nantogma, J. Ettedgui, P. Tomhon, B. M. Goodson, T. Theis, E. Y. Chekmenev, ACS Sens. 2022, 7(11), 3430–3439.
- [13] M. S. Alam, X. Li, D. O. Brittin, S. Islam, P. Deria, E. Y. Chekmenev, B. M. Goodson, *Angew. Chem. Int. Ed.* 2023, 62, e202213581.
- [14] F. Shi, A. M. M. Coffey, K. W. Waddell, E. Y. Chekmenev, B. M. Goodson, K. W. Waddell, E. Y. Chekmenev, B. M. Goodson, J. Phys. Chem. C 2015, 119, 7525–7533.
- [15] S. Min, J. Baek, J. Kim, H. Jin Jeong, J. Chung, K. Jeong, JACS Au 2023, 3, 2912–2917.
- [16] W. Iali, A. M. Olaru, G. G. R. Green, S. B. Duckett, *Chem. Eur. J.* 2017, 23, 10491–10495.
- [17] F. Shi, A. M. Coffey, K. W. Waddell, E. Y. Chekmenev, B. M. Goodson, *Angew. Chem. Int. Ed.* 2014, 53, 7495–7498.
- [18] K. V. Kovtunov, L. M. Kovtunova, M. E. Gemeinhardt, A. V. Bukhtiyarov, J. Gesiorski, V. I. Bukhtiyarov, E. Y. Chekmenev, I. V. Koptyug, B. M. Goodson, *Angew. Chem. Int. Ed.* 2017, 56, 10433–10437.
- [19] H. de Maissin, P. R. Groß, O. Mohiuddin, M. Weigt, L. Nagel, M. Herzog, Z. Wang, R. Willing, W. Reichardt, M. Pichotka, L. Heß, T. Reinheckel, H. J. Jessen, R. Zeiser, M. Bock, D. von Elverfeldt, M. Zaitsev, S. Korchak, S. Glöggler, J.-B. Hövener, E. Y. Chekmenev, F. Schilling, S. Knecht, A. B. Schmidt, Angew. Chem. Int. Ed. 2023, 62, e202306654.
- [20] K. MacCulloch, A. Browning, D. O. Guarin Bedoya, S. J. McBride, M. B. Abdulmojeed, C. Dedesma, B. M. Goodson,

- M. S. Rosen, E. Y. Chekmenev, Y.-F. Yen, P. TomHon, T. Theis, *J. Magn. Reson. Open* **2023**, *16–17*, 100129.
- [21] W. Zhang, D. P. Curran, Tetrahedron 2006, 62, 11837-11865.
- [22] Z. Luo, Q. Zhang, Y. Oderaotoshi, D. P. Curran, Science 2001, 291, 1766–1769.
- [23] D. P. Curran, S. Hadida, S.-Y. Kim, Z. Luo, D. P. Curran, S. Hadida, S.-Y. Kim, Z. Luo, J. Am. Chem. Soc. 1999, 121, 6607–6615.
- [24] E. de Wolf, G. van Koten, B.-J. Deelman, E. de Wolf, G. van Koten, B.-J. Deelman, *Chem. Soc. Rev.* 1999, 28, 37–41.
- [25] S. P. Smidt, N. Zimmermann, M. Studer, A. Pfaltz, Chem. Eur. J. 2004, 10, 4685–4693.
- [26] M. K. Tham, R. D. Walker, J. H. Modell, J. Chem. Eng. Data 1973, 18, 385–386.
- [27] C. S. M. Kang, X. Zhang, D. R. Macfarlane, J. Phys. Chem. C 2019, 123, 21376–21385.
- [28] A. Duchowny, J. Denninger, L. Lohmann, T. Theis, S. Lehmkuhl, A. Adams, *Int. J. Mol. Sci.* 2023, 24, 2465.
- [29] S. Nantogma, M. Raduanul, H. Chowdhury, M. S. H. Kabir, I. Adelabu, S. M. Joshi, A. Samoilenko, H. De Maissin, A. B. Schmidt, P. Nikolaou, Y. A. Chekmenev, O. G. Salnikov, N. V. Chukanov, I. V. Koptyug, B. M. Goodson, E. Y. Chekmenev, Anal. Chem. 2024, 96(10), 4171–4179.
- [30] J. Ettedgui, B. Blackman, N. Raju, S. A. Kotler, E. Y. Chekmenev, B. M. Goodson, H. Merkle, C. C. Woodroofe, C. A. LeClair, M. C. Krishna, R. E. Swenson, J. Am. Chem. Soc. 2023, 146, 946–953.
- [31] B. J. Tickner, O. Semenova, W. Iali, P. J. Rayner, A. C. Whitwood, S. B. Duckett, *Catal. Sci. Technol.* 2020, 10, 1343– 1355.
- [32] B. J. Tickner, J. S. Lewis, R. O. John, A. C. Whitwood, S. B. Duckett, *Dalton Trans.* 2019, 48, 15198–15206.
- [33] M. S. H. Kabir, S. M. Joshi, A. Samoilenko, I. Adelabu, S. Nantogma, J. G. Gelovani, B. M. Goodson, E. Y. Chekmenev, J. Phys. Chem. A 2023, 127, 5018–5029.
- [34] K. R. Keshari, D. M. Wilson, Chem. Soc. Rev. 2014, 43, 1627– 1659.
- [35] D. M. Wilson, R. E. Hurd, K. Keshari, M. Van Criekinge, A. P. Chen, S. J. Nelson, D. B. Vigneron, J. Kurhanewicz, *Proc. Natl. Acad. Sci. USA* 2009, 106, 5503–5507.
- [36] 3 M, "3M<sup>™</sup> Novec<sup>™</sup> 7100 Engineered Fluid," can be found under https://multimedia.3 m.com/mws/media/199818O/3 m-no-vec-7100-engineered-fluid.pdf **2009**.
- [37] T. Hune, S. Mamone, H. Schroeder, A. P. Jagtap, S. Sternkopf, G. Stevanato, S. Korchak, C. Fokken, C. A. Müller, A. B. Schmidt, D. Becker, S. Glöggler, *ChemPhysChem* 2023, 24, e202200615.
- [38] J. R. Brender, S. Kishimoto, H. Merkle, G. Reed, R. E. Hurd, A. P. Chen, J. Henrik Ardenkjaer-Larsen, J. Munasinghe, K. Saito, T. Seki, N. Oshima, K. Yamamoto, P. L. Choyke, J. Mitchell, M. C. Krishna, Sci. Rep. 2019, 9, 3410.
- [39] A. B. Schmidt, J. Eills, L. Dagys, M. Gierse, M. Keim, S. Lucas, M. Bock, I. Schwartz, M. Zaitsev, E. Y. Chekmenev, S. Knecht, A. B. Schmidt, J. Eills, L. Dagys, M. Gierse, M. Keim, S. Lucas, M. Bock, I. Schwartz, M. Zaitsev, E. Y. Chekmenev, S. Knecht, J. Phys. Chem. Lett. 2024, 15(59), 1195–1203.
- [40] C. M. Henderson, N. J. Shulman, B. MacLean, M. J. MacCoss, A. N. Hoofnagle, *Clin. Chem.* 2018, 64, 408–410.
- [41] J. D. Clark, G. F. Gebhart, J. C. Gonder, M. E. Keeling, D. F. Kohn, *ILAR J.* 1997, 38, 41–48.

Manuscript received: April 17, 2024 Accepted manuscript online: June 3, 2024 Version of record online: ■■, ■■

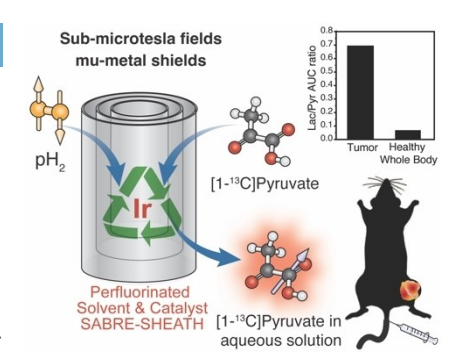
# Research Article

#### Metabolic Imaging

J. Ettedgui,\* K. Yamamoto, B. Blackman, N. Koyasu, N. Raju, O. Vasalatiy, H. Merkle, E. Y. Chekmenev, B. M. Goodson, M. C. Krishna,

e202407349 R. E. Swenson

In vivo Metabolic Sensing of Hyperpolarized [1-13C]Pyruvate in Mice Using a Recyclable Perfluorinated Iridium Signal Amplification by Reversible Exchange Catalyst



Hyperpolarization enhances pyruvate signal, enabling real-time metabolic flux monitoring by MRI. Our study presents a novel method, achieving a 22% increase in hyperpolarized in

[1-13C]pyruvate's enhancement using Signal Amplification By Reversible Exchange (SABRE) with a perfluorinated Iridium catalyst in a fluorinated solvent/methanol blend. This catalyst enables easy separation from hyperpolarized pyruvate, ensuring biocompatibility and recyclability, and allowing in vivo metabolic sensing in human pancreatic xenografts.

15213773, Q Downloaded from https://onlinelibrary.wiley.com/doi/10.1002/anie.202407349 by Reacube (Labtiva Inc.), Wiley Online Library on [06/10/2024]. See the Terms and Conditions (thtps://onlinelibrary.wiley.com/terms-and-conditions) on Wiley Online Library for rules of use; OA articles are governed by the applicable Creative Commons Licensea